American Society of Hematology
2021 L Street NW, Suite 900,
Washington, DC 20036
Phone: 202-776-0544 | Fax 202-776-0545
editorial@hematology.org

Leukemia inhibitory factor protects against graft-versus-host disease while preserving graft-versus-leukemia activity

Tracking no: BLD-2022-015677R2

Jianming Wang (Rutgers Caner Institute of New Jersey, United States) Chun-Yuan Chang (Rutgers Caner Institute of New Jersey, United States) Xue Yang (Rutgers Caner Institute of New Jersey, United States) Fan Zhou (Rutgers Caner Institute of New Jersey, United States) Juan Liu (Rutgers Caner Institute of New Jersey, United States) Sining Zhu (Department of Cell Biology and Neuroscience, Rutgers University, United States) Xue-zhong Yu (Medical College of Wisconsin, United States) Chen Liu (Yale School of Medicine, United States) Timothy E. O'Sullivan (Molecular Biology Institute, UCLA, United States) Ping Xie (Department of Cell Biology and Neuroscience, Rutgers University, United States) Zhaohui Feng (Rutgers Caner Institute of New Jersey, United States) Wenwei Hu (Rutgers Cancer Institute of New Jersey, United States)

Abstract:
Graft-versus-host disease (GVHD) remains a major complication after allogeneic hematopoietic stem cell transplantation, a widely-used therapy for hematologic malignancies and blood disorders. Here, we report an unexpected role of cytokine leukemia inhibitory factor (LIF) in protecting against GVHD development. Administrating recombinant LIF protein (rLIF) protects mice from GVHD-induced tissue damage and lethality without compromising the graft-versus-leukemia (GVL) activity, which is crucial to prevent tumor relapse. We found that rLIF reduces the infiltration and activation of donor immune cells, and protects intestinal stem cells (ISCs) to ameliorate GVHD. Mechanistically, rLIF downregulates IL12-p40 expression in recipient dendritic cells (DCs) post irradiation through activating the STAT1 signaling, which results in decreased MHC-II levels on intestinal epithelial cells and reduced donor T cell activation and infiltration. This study reveals a previously unidentified protective role of LIF for GVHD-induced tissue pathology and provides a potential effective therapeutic strategy to limit tissue pathology without compromising anti-leukemic efficacy.

Conflict of interest: No COI declared

COI notes:

Preprint server: No;

Author contributions and disclosures: J.W. carried out the experiments, analyzed data and wrote the manuscript; C.C., X. Y., F. Z., J.L., S.Z. carried out experiments; X.Y. assisted with experiments examining GVL; C. L. performed histological analysis; T.E.O. assisted with experiments analyzing IL-12 production; P.X. assisted with flow cytometric analysis of immune cell composition and activities; Z.F., W.H. designed experiments, analyzed data and wrote the manuscript.

Non-author contributions and disclosures: No;

Agreement to Share Publication-Related Data and Data Sharing Statement: For correspondence, email: fengzh@cinj.rutgers.edu (Zhaohui Feng) wh221@cinj.rutgers.edu (Wenwei Hu)

Clinical trial registration information (if any):

Leukemia inhibitory factor protects against graft-versus-host disease while preserving graft-versus-leukemia activity

Jianming Wang [1], Chun-yuan Chang [1], Xue Yang [1], Fan Zhou [1], Juan Liu [1], Sining Zhu [2], Xue-Zhong Yu [3], Chen Liu [4], Timothy E. O'Sullivan [5, 6], Ping Xie [2], Zhaohui Feng [1, *], Wenwei Hu [1, *]

1. Rutgers Cancer Institute of New Jersey, Rutgers University, New Brunswick, NJ 08903

2. Department of Cell Biology and Neuroscience, Rutgers University, Piscataway, NJ 08854

3. Department of Microbiology and Immunology, Medical College of Wisconsin, WI 53226

4. Department of Pathology, Yale School of Medicine, New Haven, CT 06520

5. Department of Microbiology, Immunology, and Molecular Genetics, David Geffen School of Medicine at UCLA, CA 90095

6. Molecular Biology Institute, UCLA, CA90095

*: Wenwei Hu, Rutgers Cancer Institute of New Jersey, New Brunswick, NJ 08903, USA. Tel: 732-235-6169; E-mail: wh221@cinj.rutgers.edu

Zhaohui Feng, Rutgers Cancer Institute of New Jersey, New Brunswick, NJ 08903, USA. Tel: 732-235-8814; E-mail: fengzh@cinj.rutgers.edu

Key Points

1. LIF protects mice against GVHD through reducing the infiltration and activation of donor immune cells, and protecting intestinal stem cells.

2. LIF decreases IL12 levels in recipient DCs and MHC-II levels on intestinal epithelium to reduce T cell activation and GVHD-induced damage.

Abstract

Graft-versus-host disease (GVHD) remains a major complication after allogeneic hematopoietic stem cell transplantation, a widely-used therapy for hematologic malignancies and blood disorders. Here, we report an unexpected role of cytokine leukemia inhibitory factor (LIF) in protecting against GVHD development. Administrating recombinant LIF protein (rLIF) protects mice from GVHD-induced tissue damage and lethality without compromising the graft-versus-leukemia (GVL) activity, which is crucial to prevent tumor relapse. We found that rLIF reduces the infiltration and activation of donor immune cells, and protects intestinal stem cells (ISCs) to ameliorate GVHD. Mechanistically, rLIF downregulates IL12-p40 expression in recipient dendritic cells (DCs) post irradiation through activating the STAT1 signaling, which results in decreased MHC-II levels on intestinal epithelial cells and reduced donor T cell activation and infiltration. This study reveals a previously unidentified protective role of LIF for GVHD-induced tissue pathology and provides a potential effective therapeutic strategy to limit tissue pathology without compromising anti-leukemic efficacy.

Introduction

Allogeneic bone marrow transplantation (allo-BMT) is a potentially curative therapy for patients with hematologic malignancies [1-3]. The therapeutic benefits of allo-BMT are derived from cytoreductive conditioning and a donor immune cell-mediated GVL effect [1-3]. However, this treatment is often limited by the development of GVHD. Acute GVHD is mainly induced by the antigen disparity between donor and recipient [1-3]. The alloreactive donor T cells, activated by host antigen-presenting cells (APCs), cause damage in vital recipient organs, classically the gastrointestinal (GI) tract, skin and liver, and initiate GVHD [1]. GVHD affects up to 70% of allo-BMT patients, with 20% to 75% mortality rates [4]. Limiting GHVD while maintaining GVL activity remains a critical goal in the clinic.

The GI tract is the main organ targeted by donor T cells during GVHD. Damage to the GI tract is the primary determinant of GVHD severity and lethality [5]. Shortly after allo-BMT, donor T cells migrate to the GI tract, and preferentially invade the crypt ISC compartment, where they damage ISCs, leading to GI injury and GVHD [6]. A recent study revealed that the elevation of cytokine interleukin 12 (IL12) levels by irradiation before allo-BMT contributes to GI injury during GVHD development [5]. The elevation of IL12 induces major histocompatibility complex class II (MHC-II) expression on the surface of intestinal epithelial cells (IECs), which serve as APCs to activate donor T cells to induce GI injury and trigger GVHD [5].

LIF was initially identified as a factor that induces the terminal differentiation of murine myeloid leukemia M1 cells (for review, see [7]). Subsequent studies revealed that LIF plays essential roles in many physiological and pathological processes, including self-renewal of pluripotent stem cells, maternal reproduction, inflammation and tumorigenesis in a highly cell-, tissue- and context-dependent manner [7]. Recently, we found that LIF is essential in maintaining

ISC number and functions to ensure the intestinal epithelial homeostasis and regeneration [8]. LIF has been reported to regulate immune response and inflammation through regulating DCs, regulatory T cells (Tregs), and macrophages under different conditions [9-11]. Considering the roles of ISC damage and inflammation in triggering GVHD [6], we investigated the role of LIF in GVHD.

In this study, we found that LIF levels are elevated at the early stage of GVHD and serum LIF levels post allo-BMT are positively correlated with the survival of mice succumbing to GVHD. Importantly, administrating rLIF protects mice from GVHD-induced tissue damage and lethality without compromising the GVL activity. rLIF reduces the infiltration and activation of donor immune cells, and protects ISCs to ameliorate GVHD. This study unveils an important role of LIF in inflammatory immune response in the context of GVHD and provides a promising therapeutic strategy for GVHD.

Methods

Mice

C57BL/6 ($H2k^b$), CD45.2 ($H2k^b$), C3H/HeJ ($H2k^k$) and BALB/c ($H2k^d$) mice were obtained from the Jackson Laboratory. B6C3F1 ($H2k^{b/k}$) mice were produced by crossing C57BL/6 mice with C3H/HeJ mice. IL12-p40-IRES-eYFP mice were generated by Dr. Richard Locksley in UCLA [12]. Conventional LIF knockout (KO) mice in C57BL/6 background were obtained from EMMA repository (EM:02619). Age- and gender-matched mice at 8-12-week-old were used for experiments in this study. Animals were randomly assigned to different treatment groups. Sample sizes were chosen based on the power calculation. For TBI treatment, mice were subjected to 11 Gy TBI with a 137 Cs γ-source irradiator at a dose rate of 90 cGy/minute. For rLIF treatment, mice were treated with intraperitoneal (*i.p.*) injection of either mouse rLIF (Millipore, 30 ng/g body weight) or PBS twice a day for different durations. For rIL12 treatment, mice were treated with *i.p.* injection of either mouse rIL12 (R&D Systems, 500 ng/day) or PBS once a day for 7 days (starting from 4 days before BMT till 3 days after BMT). The investigators were blinded to the group allocation during experiments and when assessing outcomes. All mouse experiments were approved by the Institutional Animal Care and Use Committee (IACUC) of Rutgers University.

BMT

For BMT, transplant recipients were lethally irradiated with 13 Gy TBI (split doses of 2 x 6.5 Gy with a 4 hours interval for **Fig. S4a**, **b** & lower panels of **c**) or 11 Gy TBI (if not stated otherwise, split doses of 2 x 5.5 Gy with a 4 hours interval) one day before BMT (D-1), followed by intravenous (*i.v.*) transplantation of 5 x 10^6 BM cells with or without T cells (6×10^6 for B6C3F1

recipients and 8×10^6 for C57BL/6 recipients) at day 0 (D0). Mice were monitored twice a week for body weight, GVHD score and survival.

Statistical analysis

All data were obtained from at least three repetitions and were expressed as mean ± SD or mean ± SEM as indicated in the figure legends. The survival of mice was summarized by Kaplan–Meier plots and compared by the log-rank test using the GraphPad Prism software. The body weight loss and GVHD score curve were compared by ANOVA using the GraphPad Prism software. All other *p*-values were obtained by Student's *t*-tests and Welch's correction was performed for data with big variation. Values of $p < 0.05$ were considered significant. All data points and "n" values reflect biological replicates.

All other methods are described in detail in the supplemental methods.

Results

Serum LIF levels are increased upon allo-BMT and positively correlated with the lifespan of mice with GVHD.

To investigate the potential role of LIF in GVHD, we measured serum LIF levels after allo-BMT in mice, including B6C3F1 ($H2k^{b/k}$) mice receiving allo-BMT from C57BL/6 ($H2k^{b}$) mice, a MHC-haploidentical GVHD model [13,14], and C57BL/6 ($H2k^{b}$) mice receiving allo-BMT from BALB/C ($H2k^{d}$) mice, a MHC-mismatched GVHD model [15]. Mice were irradiated with 5.5 Gy total body irradiation (TBI) twice, followed by BMT at one day after irradiation, denoted as day 0. Naïve mice, mice received TBI only, BMT from syngeneic mice (syn-BMT), and BM from allogeneic mice (allo-BM) served as controls. Serum LIF levels were significantly elevated in mice at 2 days post TBI as determined by ELISA assays (**Fig. 1a**). While syn-BMT and allo-BM induced serum LIF levels to a similar extent as TBI did, allo-BMT induced serum LIF to much higher levels, and the elevation of serum LIF levels can still be observed at 14 days and 20 days post treatments in B6C3F1 and C57BL/6 mice, respectively (**Fig. 1a**). LIF production in different tissues was examined at mRNA levels by quantitative real-time PCR (qPCR). *LIF* induction was most obvious at 2 days post treatments and then gradually declined at later time points in all tissues examined (**Fig. S1**). TBI, syn-BMT and allo-BM showed strong *LIF* induction in the colon and small intestine (SI), followed by spleen and mesenteric lymph nodes (MLNs), while allo-BMT showed very high *LIF* induction in the MLN and spleen followed by colon and SI (**Fig. S1**). Notably, in majority of tissues and time points examined, allo-BMT induced much higher levels of *LIF* than TBI, syn-BMT or allo-BM, which was consistent with the change observed in serum LIF levels (**Fig. 1a**). These results suggest that both radiation and early GVHD alloreactivity contribute to LIF induction. While B6C3F1 mice receiving allo-

BMT developed GVHD rapidly, notably, their serum LIF levels post allo-BMT were positively correlated with their lifespan post allo-BMT (**Fig. 1b**), suggesting a protective role of LIF against GVHD.

rLIF administration ameliorates GVHD in mice.

We tested the role of LIF in GVHD by employing the above-described GVHD models. B6C3F1 mice receiving allo-BMT from C57BL/6 mice developed GVHD rapidly showing severe body weight loss, increased GVHD scores (characterized by weight loss, hunching posture, skin lesions, dull fur and diarrhea) [16], and died at ~30 days post allo-BMT (**Fig. 1c**). Notably, rLIF administration (*i.p.* 30 ng/g body weight, twice/day, starting 4 days before BMT till 3 days after BMT; D-4 to D3) in B6C3F1 mice significantly ameliorated GVHD; rLIF-treated mice exhibited significantly prolonged survival, much reduced weight loss, and significantly lower GVHD scores than PBS-treated mice (**Fig. 1c**). Donor cell chimerism reached to a level of 70-95% at 7 days post allo-BMT in the spleen, MLN and lamina propria (LP) tissues in B6C3F1 mice with or without rLIF treatment as examined by flow cytometry, validating the proper donor cell chimerism (**Fig. S2**). The gating strategies of flow cytometry are shown in **Fig. S3**. The protective effect of rLIF on GVHD was also observed when rLIF was administered from D1 to D3 from BMT or even when GVHD has developed (D8 to D10 from BMT), although at a less extent compared with rLIF administration from D-4 to D3 from BMT (**Fig. 1c**). Therefore, rLIF was administered from D-4 to D3 from BMT in the following experiments. Similarly, rLIF ameliorated GVHD in C57BL/6 mice receiving allo-BMT from BALB/C mice (**Fig. 1d**). Histopathological analysis showed that multiple organs, including the SI, colon, liver, lung and skin, displayed pathological injuries in B6C3F1 mice at 14 days post allo-BMT (**Fig. 1e&f**).

These pathological injuries were markedly reduced in rLIF-treated mice (**Fig. 1e&f**). The protective effects of LIF were also observed when TBI dosage was increased to 6.5 Gy twice in both GVHD models (**Fig. S4a&b**). In C57BL/6 recipients, especially at the higher TBI dosage, rLIF exhibited the most significant protection on GVHD-induced tissue injuries in SI (**Fig. S4c**). Further, LIF deficiency in recipient mice (LIF-KO) significantly increased GVHD severity as reflected by significantly reduced survival and higher GVHD scores than wild type (WT) recipient mice (**Fig. 1g**). Together, these results demonstrate that rLIF ameliorates GVHD in mice.

rLIF reduces donor immune cell infiltration and inhibits systemic inflammation in receipt mice post BMT.

The tissue injury in GVHD is associated with inflammation, which is caused by the infiltration and activation of donor allogeneic T (allo-T) cells [1]. In both GVHD models, the mice with GVHD displayed inflammation as indicated by the swollen and increased weight of spleen and increased length of SI, which is a main organ targeted by donor T cells during GVHD [5,6] (**Fig. 2a&b**). Notably, rLIF significantly reduced inflammation in both GVHD models; compared with PBS-treated mice, rLIF-treated mice displayed much less pronounced increase of spleen weight and SI length (**Fig. 2a&b**). In B6C3F1 mice, the mRNA levels of several pro-inflammatory cytokines, including *TNFα*, *CXCL1*, *CCL2*, *IL-1a*, *IL-1b*, and *IL-22* were significantly increased in the SI at 7 days post allo-BMT as determined by qPCR (**Fig. 2c**). Notably, rLIF largely abolished the increase of these cytokine levels (**Fig. 2c**). It is worth noting that while IL-22 can display a pro-inflammatory effect and was reported to promote GVHD development [17,18], IL-22 was also shown to protect ISCs during inflammatory intestinal damage to regulate sensitivity to

GVHD [19,20], indicating the complex role of IL-22 in GVHD. Taken together, these results suggest an essential role of LIF in suppressing systemic inflammation induced by allo-BMT to prevent GVHD.

Systemic inflammation is caused by the infiltration of donor immune cells, particularly T cells [1]. We accessed the effect of rLIF on donor immune cell infiltration. The composition and number of donor immune cells were measured by flow cytometry in multiple lymphoid organs, including the spleen, MLN (an important site of immune cell activation for the SI) [3], and SI, which includes both LP (a main immune compartment of SI), and intraepithelial lymphocytes (IELs) that reside within the epithelium of the intestine (EPI) [21]. rLIF significantly reduced the number of infiltrating donor immune cells ($H2k^{k-}CD45^{+}$) in EPI represented as % of cells in the total population of intestinal cells in B6C3F1 mice at 7 days post allo-BMT (**Fig. 2d**). rLIF significantly reduced the number of infiltrating donor cells ($H2k^{k-}$ and $H2k^{d-}$ for B6C3F1 and C57BL/6 recipients, respectively), and the numbers of most types of immune cells, including $CD45^{+}$ cells, $CD4^{+}$ and $CD8^{+}$ T cells, myeloid cells (neutrophils, DCs and macrophages), and natural killer (NK) cells, in the spleen, MLN and LP in both GVHD models (**Fig. 2e&f**). This effect of rLIF on donor immune cell number was not observed in a syn-BMT C57BL/6 CD45.1 to C57BL/6 CD45.2 mouse model (**Fig. S5**). LIF was reported to promote Tregs and inhibit T helper 17 (Th17), a subset of pro-inflammatory T cells producing IL-17, under certain conditions [11,22]. We found that rLIF administration increased the percentage of Tregs in the infiltrating CD4 cells but showed no obvious effect on Th17 in the spleen, MLN and LP in B6C3F1 mice post allo-BMT (**Fig. S6**). Collectively, these results demonstrate that rLIF suppresses the infiltration of donor immune cells to inhibit systemic inflammation in mice post allo-BMT.

rLIF protects ISCs from GVHD-induced damage.

It was reported that upon allo-BMT, donor T cells were recruited to the recipient ISC compartment where they attack ISCs to initiate inflammation and subsequently GVHD [6]. Recently, we found that LIF is essential for ISC function and protects against irradiation-induced intestinal damage [8]. Here, we investigated whether the protection of ISCs by LIF contributes to its role in ameliorating GVHD. We examined the proliferation of intestinal epithelium and the number of viable ISCs in B6C3F1 mice at 2 days post allo-BMT using immunohistochemistry (IHC) staining of Ki67, a cell proliferation marker, and Olfm4, an ISC marker [8]. Allo-BMT reduced number of viable crypts (defined as a crypt-like structure containing at least five adjacent $Ki67^+$ cells) and the $Olfm4^+$ viable ISCs in the SI post allo-BMT, which was significantly rescued by rLIF administration (**Fig. 3a&b**). Interferon gamma (IFNγ), an important cytokine that induces ISC death in GVHD [23], induced death of intestinal organoids in a dose-dependent manner, which was significantly reduced by rLIF (**Fig. 3c**). These results demonstrate an important role of LIF in protecting the ISCs from allo-T cell-induced damage, contributing to the function of LIF in ameliorating GVHD.

rLIF inhibits donor T cell activation by suppressing MHC-II expression on IECs.

APCs are essential for immune response by processing and presenting antigens to lymphocytes, including T cells, to activate these cells [24]. Intriguingly, IECs can serve as APCs and play an important role in GVHD; TBI elevates MHC-II levels on IECs, which enhances donor T cell activation and leads to GVHD [5]. Indeed, a significant induction of MHC-II levels on IECs was observed in B6C3F1 and C57BL/6 mice post allo-BMT as determined by flow cytometry and Immunofluorescence (IF) staining assays (**Fig. 4a&b**). Notably, rLIF suppressed the antigen

presenting function of IECs by significantly reducing MHC-II induction on IECs post allo-BMT (**Fig. 4a**&**b**). rLIF showed no obvious effect on MHC-II expression on macrophages and DCs in spleen and MLNs (**Fig. S7a**). IFNγ induced MHC-II expression on IECs in intestinal organoids (**Fig. S7b**), which is consistent with previous reports [25,26]. rLIF showed no obvious effect on IFNγ-induced MHC-II expression in intestinal organoids (**Fig. S7b**), excluding the possibility that LIF directly regulates MHC-II expression on IECs. In line with the reduced MHC-II levels, rLIF greatly reduced the number of activated donor T cells ($CD25^+/CD69^+/KLRG1^+$ cells [27,28]) (**Fig. 4c**). These results demonstrate that LIF inhibits MHC-II expression on IECs post allo-BMT, which in turn reduces donor T cell activation.

rLIF suppresses IL12 production in recipient DCs to inhibit Th1 differentiation and protect against GVHD.

MLNs are crucial in regulating the immune microenvironment of the SI [3]. We compared the cytokines released from MLNs post TBI between mice with and without rLIF administration. TBI (11 Gy) in C57BL/6 mice led to a reduction of many immune cell types in MLNs due to cell death at 24 hours post TBI, which is the time to perform BMT (**Fig. S8a**). Notably, TBI did not change DC numbers in MLNs (**Fig. S8a)**. We measured the mRNA levels of cytokines in DCs isolated from MLNs post TBI by using a Nanostring myeloid innate immunity gene expression panel. TBI altered the cytokine expression patterns in DCs (**Fig. S8b**). *IL12b* encoding IL12-p40, a well-known inflammatory cytokine, stood out with obvious induction by TBI in DCs, and its induction was largely reduced by rLIF (**Fig. S8b**). Consistently, IL12-p40 was greatly induced by TBI in DCs, and its induction was significantly reduced by rLIF as analyzed by using a cytokine array measuring the protein levels of cytokines in DCs (**Fig. 5a**&**S8c**). This finding

was validated by using the IL12-p40-IRES-eYFP (IL12-p40-YFP) mouse model, which has a knock-in allele expressing YFP from the IL12-p40 locus and can be used to measure IL12-p40 production *in vivo* [29]. TBI greatly increased the percentage and number of IL12-p40-YFP$^+$ DCs, which were significantly reduced by rLIF (**Fig. 5b**&**S8d**). Consistently, TBI increased IL12-p40 levels in MLNs and serum as measured by ELISA assays, which were significantly reduced by rLIF (**Fig. S8e**). Bioactive IL12 (IL12-p70), which is required for IFNγ production and T help 1 (Th1) cell differentiation, is a 70-kDa heterodimer protein composed of 2 subunits: p35 and p40 [30]. Consistent with the results of IL12-p40, TBI increased IL12-p70 levels in MLNs, which was largely abolished by rLIF (**Fig. S8f**). rLIF had no obvious effect on the levels of IL-23, another important cytokine for GVHD pathology that shares the IL12-p40 subunit with IL12 [31] (**Fig. S8g**). IL12-p40 can be produced by DCs and macrophages [30]. We found that DCs but not macrophages were the predominant cell type that produces IL12-p40 in MLNs (**Fig. S8d**).

We examined whether the inhibitory effect of rLIF on IL12-p40 induction by TBI suppresses donor Th1 differentiation post allo-BMT. The expression of the transcription factor T-bet in CD4$^+$ T cells is a hallmark of Th1 differentiation [5]. Notably, in B6C3F1 mice with allo-BMT, T-bet levels in donor CD4$^+$ T cells were much lower in MLNs from rLIF-treated mice than PBS-treated mice (**Fig. 5c**). Consistently, the mRNA levels of *IFNγ*, encoding a well-known Th1 cytokine [32], in SI, protein levels of IFNγ in SI and serum, and the numbers of infiltrating donor CD4$^+$ IFNγ$^+$ cells in MLNs, were much lower in rLIF-treated mice than PBS-treated mice (**Fig. 5d**&**S9a**). rLIF had no obvious effect on Th1 differentiation *in vitro* (**Fig. S9b**&**c**), excluding the possibility the LIF directly inhibits Th1 differentiation.

IL12 was recently reported to induce MHC-II expression on IECs upon TBI [5]. Here, we tested whether the inhibitory effect of LIF on TBI-induced IL12 contributes to the inhibitory

effect of LIF on the increase of MHC-II level on IECs induced TBI and subsequent protection against GVHD. B6C3F1 mice with allo-BMT were administered with recombinant IL12 protein (rIL12). Intriguingly, rIL12 largely abolished the protective effect of rLIF on GVHD, as indicated by the increased spleen weight and SI length, elevated MHC-II expression on IECs, enhanced infiltration of donor immune cells in the spleen, MLN and LP tissues in mice receiving allo-BMT along with rLIF and rIL12 treatments compared with mice receiving allo-BMT and rLIF treatment (**Fig. 5e-h**). In contrast, rIL12 exhibited a very limited effect on mice receiving allo-BMT without rLIF treatment (**Fig. 5e-h**). These results indicate that the regulation of IL12 levels by LIF mediates the protective effect of LIF on GVHD.

rLIF regulates IL12 in DCs through the STAT1 signaling.

To study the mechanism whereby LIF regulates IL12 production in DCs, we employed BM-derived DCs (BMDCs) as an *in vitro* model [33]. IFNγ and lipopolysaccharides (LPS) were used to stimulate BMDCs, which mimics radiation-induced inflammatory microenvironment. IFNγ and LPS treatment significantly increased *IL12b* production in BMDCs, which was largely abolished by rLIF (**Fig. 5i**). This is consistent with the results from our *in vivo* experiments showing that rLIF reduced IL12-p40 production from DCs post TBI (**Fig. 5a**, **b**, **S8b-d**). LIF exerts its function through selectively activating its downstream pathways in a highly tissue- and cell-type specific manner [7]. We examined a panel of well-known LIF downstream pathways, including the STATs, AKT, ERK and MAPK pathways [7], in BMDCs derived from C57BL/6 and B6C3F1 upon IFNγ and LPS stimulation. rLIF greatly enhanced STAT1 activity as reflected by the increased levels of STAT1 phosphorylation at Tyr-701 (p-STAT1) but not the total STAT1 protein levels in BMDCs treated with IFNγ and LPS (**Fig. 5j**&**S10a**). No clear activation of

297 other major signaling pathways was observed in BMDCs upon rLIF treatment (**Fig. 5j**&**S10a**).
298 The specificity of the antibodies was validated in **Fig. S10b**&**c**. As a transcription factor, STAT1
299 mainly exerts its function through binding to the promoter region of its target genes to activate or
300 repress their transcription [34,35]. The signaling through STAT proteins plays complex roles in DC
301 activation. Currently, the role of STAT1 in IFNγ and LPS-induced IL12-p40 expression is
302 unclear. It was reported that the STAT1 signaling inhibits CD40L-induced IL-12 production in
303 DCs [36]. Here, we investigated whether LIF regulates IL12-p40 production in BMDCs through
304 the transcriptional regulation by STAT1. A putative STAT-binding *cis*-acting element [37,38] was
305 identified in the intron 1 of the mouse *IL12b* gene encoding IL12-p40 (**Fig. 5k**). Chromatin
306 immunoprecipitation (ChIP) assays showed that rLIF significantly enhanced the binding of
307 STAT1 to the regulatory region of *IL12b* containing the potential STAT1-binding elements in
308 BMDCs activated by IFNγ and LPS (**Fig. 5k**). Furthermore, blocking the STAT1 function in
309 BMDCs by two small-molecule STAT1 inhibitors, fludarabine [39] and pravastatin [40], greatly
310 abolished the inhibitory effect of rLIF on *IL12b* expression in BMDCs, and showed a much less
311 pronounced effect on *IL12b* expression in BMDCs without LIF treatment (**Fig. 5l**).
312 Collectively, these results suggest that LIF inhibits IL12-p40 production in DCs upon
313 inflammatory stimulation mainly through the STAT1 signaling.
314
315 **rLIF preserves the GVL effect.**
316 Although responsible for GVHD, allo-T cells play a key role in eliminating residual leukemia
317 cells to prevent tumor relapse (known as GVL), which is the key to the success of BMT [2]. Here,
318 we determined whether rLIF affects GVL by employing the BALB/C to C57BL/6 BMT model
319 supplemented with C1498 murine acute myeloid leukemia cells with a luciferase reporter

transduced for bioluminescence imaging (BLI) tumor tracking, which is a well-established GVL model [41]. The recipient mice with BM and C1498 cells quickly succumbed to leukemia with strong BLI signals reflecting leukemia development, and all mice died by 28 days post BMT (**Fig. 6a-c**). rLIF inhibited and delayed leukemia growth and prolonged the survival of mice receiving BM and C1498 cells by ~5 days (**Fig. 6a-c**). While the addition of allo-T cells largely prevented leukemia relapse in mice with allo-BMT, these mice had GVHD as a major cause of mortality with a medium lifespan of ~ 50 days post allo-BMT (**Fig. 6a-c**). Importantly, rLIF significantly improved the survival of mice with allo-BMT; over 50% of mice were still alive at the end of the experiment at 80 days post allo-BMT (**Fig. 6a**). These results indicate that rLIF administration alleviates GVHD, and at the same time, preserves the GVL activity (**Fig. 6d**).

Discussion

LIF plays important roles in many physiological and pathological conditions (for review, see refs. [7,42]). However, the role of LIF in immune cell- and inflammation-caused damage in the context of GVHD remains unknown. In this study, by employing preclinical GVHD mouse models, we demonstrated that serum LIF levels were significantly elevated in mice receiving allo-BMT and the serum LIF levels post allo-BMT were positively correlated with the survival of mice post allo-BMT that succumbed to GVHD. While these results indicate the potential protecting effect of LIF on GVHD, the fact that mice receiving allo-BMT developed GVHD indicates that additional LIF is needed to protect against GVHD. Indeed, rLIF administration for a relative short period significantly protected mice from GVHD and prolonged mouse lifespan. In line with our findings in mice, analysis of a publicly available dataset of transcriptome sequencing of rectosigmoid biopsies from GVHD patients (GSE134662, [43]) revealed a trend in reduction (16 out of 22 patients) of LIF levels in the colon of patients with refractory GVHD compared to LIF levels at the time of GVHD onset (**Fig. S11**), suggesting that colon LIF levels are correlated with GVHD progression and has the potential to be developed as a biomarker for GVHD. However, the patient size in this dataset is relatively small, future studies including more patients and normal control populations are needed for validation.

Damage to the GI tract is the main determinant of GVHD severity and lethality [5]. Upon allo-BMT, donor T cells are recruited to the intestinal crypt region to attack ISCs [6]. These findings highlight the importance of ISC protection for GVHD therapeutics. Results from this study demonstrated that rLIF promoted the ISC regeneration and proliferation post allo-BMT, suggesting that the effect of LIF on the ISC compartment contributes to the protective role of LIF in GVHD.

Allo-T cells infiltrate into recipient tissues post allo-BMT and get activated by APCs, which leads to inflammation and subsequent tissue damage and lethality in GVHD [5]. A recent study reported that IECs act as APCs to induce donor T cell activation and GVHD initiation [5]. Here, we demonstrated that rLIF reduced the inflammation and donor T cell infiltration in GVHD. IL12 is a key inflammatory cytokine and inducer of GVHD [5,44]. Our results showed that rLIF reduced IL12-p40 induction by TBI in recipient DCs in MLNs, which then reduced MHC-II expression on IECs to inhibit Th1 differentiation and donor T cell activation. rIL12 administration largely abolished the protective effect of rLIF. Thus, our results revealed a previously unidentified role of LIF in regulating IL12 expression, constituting a critical mechanism whereby LIF exerts its protective role in GVHD. The STAT family consists of seven transcription factors [45]. Previous studies, including ours, demonstrate STAT3 as a critical LIF downstream target in regulating many biological processes [46-49]. LIF also promotes STAT4 activation to reduce intestinal inflammation in a mouse colitis model [50]. Here, we found that LIF activated STAT1 in BMDCs to transcriptionally repress IL12-p40. These results suggest a cell/tissue-type and context-specific role of LIF in regulating its downstream pathways to modulate different biological and pathological processes. STAT1 knockout mice can be employed to validate the role of LIF in DCs in future studies.

Despite GVHD, allo-T cells remain the key to the success of BMT due to their GVL activity. Of clinical importance, we evaluated the impact of LIF upon donor T cell-mediated GVL activity. Notably, LIF not only reduced GVHD, but also preserved GVL activity, supporting the potential of LIF as a therapeutic agent to protect against GVHD while preserving GVL. While allogeneic donor Th1 cells were shown to induce both GVHD and GVL in mouse models, it was reported that Th1 blockade by targeting T-bet ameliorates GVHD without

decreasing GVL activity, indicating the differential sensitivity of GVHD and GVL to Th1 reduction [51]. Our results showed that LIF inhibited but did not completely block Th1 and T cell activation, which could be the reason for LIF to protect against GVHD while preserving GVL.

Taken together, this study revealed a crucial role of LIF in protecting against GHVD by supporting ISC function and inhibiting donor T cell infiltration and activation *via* modulating the STAT1/IL12/MHC-II axis. Our results suggest a potential translational application of LIF as a therapeutic agent to protect against GVHD while preserving GVL.

References

1. Zeiser R, Blazar BR. Acute Graft-versus-Host Disease - Biologic Process, Prevention, and Therapy. *N Engl J Med*. 2017;377(22):2167-2179.
2. Gyurkocza B, Sandmaier BM. Conditioning regimens for hematopoietic cell transplantation: one size does not fit all. *Blood*. 2014;124(3):344-353.
3. Koyama M, Hill GR. The primacy of gastrointestinal tract antigen-presenting cells in lethal graft-versus-host disease. *Blood*. 2019;134(24):2139-2148.
4. Paczesny S. Biomarkers for posttransplantation outcomes. *Blood*. 2018;131(20):2193-2204.
5. Koyama M, Mukhopadhyay P, Schuster IS, et al. MHC Class II Antigen Presentation by the Intestinal Epithelium Initiates Graft-versus-Host Disease and Is Influenced by the Microbiota. *Immunity*. 2019;51(5):885-898 e887.
6. Fu YY, Egorova A, Sobieski C, et al. T Cell Recruitment to the Intestinal Stem Cell Compartment Drives Immune-Mediated Intestinal Damage after Allogeneic Transplantation. *Immunity*. 2019;51(1):90-103 e103.
7. Zhang C, Liu J, Wang J, Hu W, Feng Z. The emerging role of leukemia inhibitory factor in cancer and therapy. *Pharmacol Ther*. 2021;221:107754.
8. Wang H, Wang J, Zhao Y, et al. LIF is essential for ISC function and protects against radiation-induced gastrointestinal syndrome. *Cell Death Dis*. 2020;11(7):588.
9. Yaftiyan A, Eskandarian M, Jahangiri AH, Kazemi Sefat NA, Moazzeni SM. Leukemia inhibitory factor (LIF) modulates the development of dendritic cells in a dual manner. *Immunopharmacol Immunotoxicol*. 2019;41(3):455-462.
10. Jeannin P, Duluc D, Delneste Y. IL-6 and leukemia-inhibitory factor are involved in the generation of tumor-associated macrophage: regulation by IFN-gamma. *Immunotherapy*. 2011;3(4 Suppl):23-26.
11. Janssens K, Van den Haute C, Baekelandt V, et al. Leukemia inhibitory factor tips the immune balance towards regulatory T cells in multiple sclerosis. *Brain Behav Immun*. 2015;45:180-188.
12. Reinhardt RL, Hong S, Kang SJ, Wang ZE, Locksley RM. Visualization of IL-12/23p40 in vivo reveals immunostimulatory dendritic cell migrants that promote Th1 differentiation. *J Immunol*. 2006;177(3):1618-1627.
13. Nabekura T, Shibuya K, Takenaka E, et al. Critical role of DNAX accessory molecule-1 (DNAM-1) in the development of acute graft-versus-host disease in mice. *Proc Natl Acad Sci U S A*. 2010;107(43):18593-18598.
14. Inoue T, Ikegame K, Kaida K, et al. Host Foxp3+CD4+ Regulatory T Cells Act as a Negative Regulator of Dendritic Cells in the Peritransplantation Period. *J Immunol*. 2016;196(1):469-483.
15. Lee SM, Park HY, Suh YS, et al. Inhibition of acute lethal pulmonary inflammation by the IDO-AhR pathway. *Proc Natl Acad Sci U S A*. 2017;114(29):E5881-E5890.
16. Lamarthee B, Marchal A, Charbonnier S, et al. Transient mTOR inhibition rescues 4-1BB CAR-Tregs from tonic signal-induced dysfunction. *Nat Commun*. 2021;12(1):6446.
17. Zhao K, Zhao D, Huang D, et al. Interleukin-22 aggravates murine acute graft-versus-host disease by expanding effector T cell and reducing regulatory T cell. *J Interferon Cytokine Res*. 2014;34(9):707-715.

18. Lamarthee B, Malard F, Gamonet C, et al. Donor interleukin-22 and host type I interferon signaling pathway participate in intestinal graft-versus-host disease via STAT1 activation and CXCL10. *Mucosal Immunol*. 2016;9(2):309-321.
19. Lindemans CA, Calafiore M, Mertelsmann AM, et al. Interleukin-22 promotes intestinal-stem-cell-mediated epithelial regeneration. *Nature*. 2015;528(7583):560-564.
20. Hanash AM, Dudakov JA, Hua G, et al. Interleukin-22 protects intestinal stem cells from immune-mediated tissue damage and regulates sensitivity to graft versus host disease. *Immunity*. 2012;37(2):339-350.
21. Cheroutre H, Lambolez F, Mucida D. The light and dark sides of intestinal intraepithelial lymphocytes. *Nat Rev Immunol*. 2011;11(7):445-456.
22. Cao W, Yang Y, Wang Z, et al. Leukemia inhibitory factor inhibits T helper 17 cell differentiation and confers treatment effects of neural progenitor cell therapy in autoimmune disease. *Immunity*. 2011;35(2):273-284.
23. Takashima S, Martin ML, Jansen SA, et al. T cell-derived interferon-gamma programs stem cell death in immune-mediated intestinal damage. *Sci Immunol*. 2019;4(42).
24. Yang W, Deng H, Zhu S, et al. Size-transformable antigen-presenting cell-mimicking nanovesicles potentiate effective cancer immunotherapy. *Sci Adv*. 2020;6(50).
25. Wosen JE, Ilstad-Minnihan A, Co JY, et al. Human Intestinal Enteroids Model MHC-II in the Gut Epithelium. *Front Immunol*. 2019;10:1970.
26. Van Der Kraak LA, Schneider C, Dang V, et al. Genetic and commensal induction of IL-18 drive intestinal epithelial MHCII via IFNgamma. *Mucosal Immunol*. 2021;14(5):1100-1112.
27. Herndler-Brandstetter D, Ishigame H, Shinnakasu R, et al. KLRG1(+) Effector CD8(+) T Cells Lose KLRG1, Differentiate into All Memory T Cell Lineages, and Convey Enhanced Protective Immunity. *Immunity*. 2018;48(4):716-729 e718.
28. Edwards J, Wilmott JS, Madore J, et al. CD103(+) Tumor-Resident CD8(+) T Cells Are Associated with Improved Survival in Immunotherapy-Naive Melanoma Patients and Expand Significantly During Anti-PD-1 Treatment. *Clin Cancer Res*. 2018;24(13):3036-3045.
29. Garris CS, Arlauckas SP, Kohler RH, et al. Successful Anti-PD-1 Cancer Immunotherapy Requires T Cell-Dendritic Cell Crosstalk Involving the Cytokines IFN-gamma and IL-12. *Immunity*. 2018;49(6):1148-1161 e1147.
30. Tait Wojno ED, Hunter CA, Stumhofer JS. The Immunobiology of the Interleukin-12 Family: Room for Discovery. *Immunity*. 2019;50(4):851-870.
31. Das R, Chen X, Komorowski R, Hessner MJ, Drobyski WR. Interleukin-23 secretion by donor antigen-presenting cells is critical for organ-specific pathology in graft-versus-host disease. *Blood*. 2009;113(10):2352-2362.
32. Cope A, Le Friec G, Cardone J, Kemper C. The Th1 life cycle: molecular control of IFN-gamma to IL-10 switching. *Trends Immunol*. 2011;32(6):278-286.
33. Roney K. Bone Marrow-Derived Dendritic Cells. *Methods Mol Biol*. 2019;1960:57-62.
34. Mizoguchi Y, Okada S. Inborn errors of STAT1 immunity. *Curr Opin Immunol*. 2021;72:59-64.
35. Totten SP, Im YK, Cepeda Canedo E, et al. STAT1 potentiates oxidative stress revealing a targetable vulnerability that increases phenformin efficacy in breast cancer. *Nat Commun*. 2021;12(1):3299.
36. Longman RS, Braun D, Pellegrini S, Rice CM, Darnell RB, Albert ML. Dendritic-cell maturation alters intracellular signaling networks, enabling differential effects of IFN-alpha/beta on antigen cross-presentation. *Blood*. 2007;109(3):1113-1122.

37. Pramanik R, Jorgensen TN, Xin H, Kotzin BL, Choubey D. Interleukin-6 induces expression of Ifi202, an interferon-inducible candidate gene for lupus susceptibility. *J Biol Chem*. 2004;279(16):16121-16127.
38. He F, Ge W, Martinowich K, et al. A positive autoregulatory loop of Jak-STAT signaling controls the onset of astrogliogenesis. *Nat Neurosci*. 2005;8(5):616-625.
39. Liu W, Miao C, Zhang S, et al. VAV2 is required for DNA repair and implicated in cancer radiotherapy resistance. *Signal Transduct Target Ther*. 2021;6(1):322.
40. Miklossy G, Hilliard TS, Turkson J. Therapeutic modulators of STAT signalling for human diseases. *Nat Rev Drug Discov*. 2013;12(8):611-629.
41. Fu J, Wu Y, Nguyen H, et al. T-bet Promotes Acute Graft-versus-Host Disease by Regulating Recipient Hematopoietic Cells in Mice. *J Immunol*. 2016;196(7):3168-3179.
42. Yue X, Wu L, Hu W. The regulation of leukemia inhibitory factor. *Cancer Cell Microenviron*. 2015;2(3):e877.
43. Holtan SG, Shabaneh A, Betts BC, et al. Stress responses, M2 macrophages, and a distinct microbial signature in fatal intestinal acute graft-versus-host disease. *JCI Insight*. 2019;5:e129762.
44. Bastian D, Wu Y, Betts BC, Yu XZ. The IL-12 Cytokine and Receptor Family in Graft-vs.-Host Disease. *Front Immunol*. 2019;10:988.
45. Villarino AV, Kanno Y, O'Shea JJ. Mechanisms and consequences of Jak-STAT signaling in the immune system. *Nat Immunol*. 2017;18(4):374-384.
46. Niwa H, Ogawa K, Shimosato D, Adachi K. A parallel circuit of LIF signalling pathways maintains pluripotency of mouse ES cells. *Nature*. 2009;460(7251):118-122.
47. Liang XH, Deng WB, Li M, et al. Egr1 protein acts downstream of estrogen-leukemia inhibitory factor (LIF)-STAT3 pathway and plays a role during implantation through targeting Wnt4. *J Biol Chem*. 2014;289(34):23534-23545.
48. Yue X, Zhao Y, Zhang C, et al. Leukemia inhibitory factor promotes EMT through STAT3-dependent miR-21 induction. *Oncotarget*. 2016;7(4):3777-3790.
49. Yu H, Yue X, Zhao Y, et al. LIF negatively regulates tumour-suppressor p53 through Stat3/ID1/MDM2 in colorectal cancers. *Nat Commun*. 2014;5:5218.
50. Zhang YS, Xin DE, Wang Z, et al. STAT4 activation by leukemia inhibitory factor confers a therapeutic effect on intestinal inflammation. *EMBO J*. 2019;38(6):e99595.
51. Yu Y, Wang D, Liu C, et al. Prevention of GVHD while sparing GVL effect by targeting Th1 and Th17 transcription factor T-bet and RORgammat in mice. *Blood*. 2011;118(18):5011-5020.

Acknowledgements

W.H. is supported by the grants from NIH R01CA203965, R01CA260838, DoD W81XWH-18-10238 and NJCCR COCR22PRG004. Z.F. is supported by the grants from NIH R01CA227912 and R01CA214746. P.X. is supported by the grant from NIH R21AI128264. This study was also supported by the Flow Cytometry/Cell Sorting shared resource of Rutgers Cancer Institute of New Jersey (NIH P30CA072720).

Author contributions

J.W. carried out the experiments, analyzed data and wrote the manuscript; C.C., X. Y., F. Z., J.L., S.Z. carried out experiments; X.Y. assisted with experiments examining GVL; C. L. performed histological analysis; T.E.O. assisted with experiments analyzing IL-12 production; P.X. assisted with flow cytometric analysis of immune cell composition and activities; Z.F., W.H. designed experiments, analyzed data and wrote the manuscript.

Competing interests

Authors declare no competing interests.

Figure legends

Figure 1. Administering rLIF ameliorates GVHD in mice.

a. Serum LIF levels in B6C3F1 (left panel) and C57BL/6 (right panel) mice at different days (D) post TBI (2 × 5.5 Gy), syngeneic BM + T, allogenic BM, and allogenic BM + T. n ≥ 3 mice/group (each dot represents a mouse). Serum LIF levels were measured by ELISA assays.

b. The serum LIF levels at 2 days post allo-BMT were positively correlated with the survival length of mice post allo-BMT. B6C3F1 mice were exposed to 2 × 5.5 Gy TBI, followed by transplantation of BM and T cells from C57BL/6 mice.

c. Lethally irradiated B6C3F1 mice received BM alone (BM; n=3), BM and T cells from C57BL/6 mice (BM + T; n=13), or BM and T cells along with rLIF treatment (*i.p.*, 30 ng/g body weight, twice a day for the period as indicated) (BM + T + rLIF; n=10 for D-4 to D3; n=8 for D1 to D3 and D8 to D10). Schematic diagram of experimental procedures is shown on the left. Three panels shown are Kaplan-Meier survival curves (left), weight loss (middle) and GVHD score (right) of mice post allo-BMT.

d. Lethally irradiated C57BL/6 mice received BM (n=3), BM + T from BALB/c mice (n=12), or BM + T + rLIF (n=9). rLIF was treated as following: *i.p.*, 30 ng/g body weight, twice a day for 7 days (D-4 to D3). Three panels shown are Kaplan-Meier survival curves (left), weight loss (middle) and GVHD score (right) of mice post allo-BMT.

e & **f.** Tissues from lethally irradiated B6C3F1 mice receiving C57BL/6 BM (n=4), BM + T (n=8) or BM + T + rLIF (n=8). Tissues from these mice were collected at 14 days post allo-BMT for histopathologic analysis. **e**: Representative H&E images of SI, colon, and liver tissues. **f**: The clinical score was analyzed as described in Methods for histopathologic damage in different tissues.

g. Lethally irradiated C57BL/6 WT (n=11) and LIF-KO (n=7) mice received BM + T from BALB/c mice. Kaplan-Meier survival curves (left) and GVHD score (right) of mice post allo-BMT are presented.

Data presented are from at least 3 independent experiments. For **a** & **f**, data are presented as mean ± SD; for **c, d** & **g**, data are presented as mean ± SEM. *: $p < 0.05$, **: $p < 0.01$, ***: $p < 0.001$, n.s.: not significant; unpaired *t*-test with Welch's correction for **a** and **f,** Spearman's correlation for **b**, Kaplan-Meier survival analysis for survival, and ANOVA for analysis of weight loss & GVHD score.

Figure 2. rLIF administration reduces tissue inflammation and donor immune cell infiltration post allo-BMT.

Lethally irradiated B6C3F1 and C57BL/6 mice received BM, BM + T cells from C57BL/6 and BALB/c mice, respectively, along with or without rLIF treatment.

a & **b.** BM+T increased spleen weight (**a**) and length of SI (**b**) in B6C3F1 mice and C57BL/6 mice at 7 days and 10 days post allo-BMT, respectively, which was largely abolished by rLIF administration. Left panel in **a**: representative images of spleen tissues. For B6C3F1 mice: n = 4 for BM; n = 16 for both BM + T and BM + T + rLIF; for C57BL/6 mice: $n \geq 4$ for BM; $n \geq 5$ for both BM + T and BM + T + rLIF.

c. rLIF administration reduced the expression of majority inflammatory cytokines examined in B6C3F1 mice at 7 days post allo-BMT. Relative mRNA expression levels of *TNFα*, *CXCL1*, *CCL2*, *IL-1a*, *IL-1b*, and *IL-22* in SI were determined by qPCR assays and normalized with *β-actin*. $n \geq 5$ mice/group.

d. rLIF administration reduced the infiltration of donor $CD45^+$ immune cells in EPI from B6C3F1 mice at 7 days post allo-BMT. Representative flow cytometry images (left panels) and quantifications (right) show the percentage of donor $CD45^+$ immune cells ($H2k^{k-}CD45^+$) in EPI from B6C3F1 mice at 7 days post allo-BMT. n = 8 mice/group.

e & **f**. rLIF administration reduced the donor immune cell infiltration in B6C3F1 (left panels) and C57BL/6 (right panels) mice at 7 days and 10 days post allo-BMT, respectively. **e**. The numbers of infiltrating donor cells in spleen, MLN, and LP tissues determined by flow cytometric assays. **f**. The numbers of a set of infiltrating donor immune cells, including CD45, CD4, CD8, Neutrophil, DC, Macrophage and NK, in spleen (upper panel), MLN (middle panel), and LP (lower panel) tissues. The number of cells in mice received BM+T without rLIF treatment was defined as 1. Gating strategies are shown in **Fig. S3**. $n \geq 7$ mice/group.

Data are presented as mean ± SD from at least 3 independent experiments. *: $p < 0.05$, **: $p < 0.01$, ***: $p < 0.001$, unpaired *t*-test with Welch's correction.

Figure 3. rLIF administration protects ISCs from GVHD-induced damage.

a & **b**. Administration of rLIF significantly increased the number of proliferating crypts (**a**) and viable ISCs (**b**) in B6C3F1 mice at 2 days post allo-BMT. Left panels: representative images of IHC staining of Ki67 (**a**) and Olfm4 (**b**) in the duodenum and ileum tissues. Right panels: quantification of viable crypts/field (**a**) and Olfm4 positive crypts/field (**b**) in the duodenum and ileum of mice post allo-BMT. n = 30 fields from at least 3 mice/group.

c. IFNγ induced cell death in intestinal organoids derived from B6C3F1 mice, which was largely reduced by rLIF. Left panels: representative images of organoid growth; right panel: quantification of organoid viability. n = 4/group.

Data are presented as mean ± SD. ***: $p < 0.001$, n.s.: not significant. Student's *t*-test.

Figure 4. rLIF administration inhibits the elevation of MHC-II expression on IECs and donor T cell activation post allo-BMT.

a & **b.** Allo-BMT increased MHC-II presentation on IECs, which was reduced by administering rLIF in mice.

a: Left panels: representative histograms (left) and quantifications of mean florescence intensity (MFI) (right) of MHC-II levels on IECs from B6C3F1 mice at 7 days post allo-BMT. Right panels: representative histograms (left) and quantifications of MFI (right) of MHC-II levels on IECs from C57BL/6 mice at 10 days post allo-BMT. For B6C3F1 recipients, n = 3 for BM; n = 8 for both BM + T and BM + T + rLIF; for C57BL/6 recipients, n = 3 for BM; n = 10 for both BM + T and BM + T + rLIF.

b: Left panels: representative IF staining of MHC-II levels on IECs in the SI from C57BL/6 mice at different days post allo-BMT. Right panel: quantifications of MHC-II MFI. $n \geq 3$ mice/group.

c. The numbers of donor activated T cells in the MLN (upper) and LP (lower) tissues from B6C3F1 mice at 7 days post allo-BMT with or without rLIF administration. $n \geq 8$ mice/group.

Data are presented as mean ± SD. *: $p < 0.05$, **: $p < 0.01$, ***: $p < 0.001$, unpaired *t*-test with Welch's correction.

Figure 5. rLIF administration inhibits radiation-induced IL12 production in DCs through the STAT1 signaling to protect against GVHD.

a. TBI (11 Gy) induced IL12 production from DCs in MLNs, which was greatly reduced by rLIF administration as examined by using the cytokine panel at 24 hours post TBI in C57BL/6 mice. n = 8 mice/group.

b. TBI (11 Gy) increased percentage (left) and number (right) of $IL12^+$ cells in DCs in MLNs at 24 hours post TBI, which were largely reduced by rLIF administration in IL12-p40-YFP C57BL/6 reporter mice as examined by flow cytometric assays. $n \geq 4$ mice/group. The gating strategy and representative flow images are shown in **Fig. S8d**.

c. The significantly reduced expression of T-bet in donor $CD4^+$ T cells in MLNs from B6C3F1 mice at 7 days post allo-BMT with rLIF administration compared with mice without rLIF administration as determined by flow cytometric assays. n = 8 mice/group.

d. The induction of the expression of Th1 cytokine IFNγ by BM+T in B6C3F1 mice was largely reduced by rLIF administration as determined at 7 days post allo-BMT. Left panel: relative mRNA expression levels of *IFNγ* in the SI determined by qPCR assays. Middle and right panels: protein levels of IFNγ in the SI (middle panel) and serum (right panel) determined by ELISA assays. $n \geq 4$ mice/group.

e & **f.** Administering rIL12 largely abolished the protective effect of rLIF on GVHD. Lethally irradiated B6C3F1 mice received allo-BMT from C57BL/6 mice along with or without rLIF administration were treated with rIL12 (500 ng/day for 7 days from D-4 to D3) or PBS. **e.** The spleen weight (left) and length of SI (right) in B6C3F1 mice measured at 7 days post allo-BMT. **f.** MFI of MHC-II on IECs of B6C3F1 mice determined at 7 days post allo-BMT. $n \geq 3$ mice/group.

g & **h.** Administering rIL12 largely abolished the inhibitory effect of rLIF on donor immune cell infiltration post allo-BMT. **g**. The relative numbers of infiltrating donor cells in the spleen, MLN, and LP tissues from B6C3F1 mice at 7 days post allo-BMT. **h**. The relative numbers of infiltrating donor immune cells in the spleen (upper), MLN (middle) and LP (lower) tissues from B6C3F1 mice at 7 days post allo-BMT. $n \geq 6$ mice/group.

i. BMDCs were activated by IFNγ (10 ng/ml) and LPS (100 ng/ml) along with or without LIF treatment (100 ng/ml) for 6 hours. The mRNA levels of *IL12b* in BMDCs were determined by qPCR assays and normalized with *β-actin*. n = 7/group.

j. rLIF treatment increased the phosphorylation levels of STAT1 at Tyr-701 (p-STAT1) in activated BMDC as determined by Western-blot assays.

k. rLIF treatment increased the binding of STAT1 to a putative STAT1 binding site in the intron 1 of *IL12b* gene as determined in BMDCs by ChIP assays. Top panel shows the sequence and location of the putative STAT1 binding site in *IL12b* gene. A region containing no STAT1 binding site was included as a negative control. n = 5/group. n.d.: non-detectable.

l. Blocking the STAT1 signaling by Fludarabine (2 μM) and Pravastatin (2 μM), two small-molecule STAT1 inhibitors, largely abolished the inhibitory effect of rLIF on IL12b production in activated BMDCs. The mRNA levels of *IL12b* in BMDCs were determined by qPCR assays and normalized with *β-actin*. n = 3/group.

Data are presented as mean ± SD from 3 independent experiments. *: $p < 0.05$, **: $p < 0.01$, ***: $p < 0.001$, n.s.: not significant; unpaired *t*-test with Welch's correction.

Figure 6. rLIF administration effectively ameliorates GVHD and preserves the GVL effect.

a-c. Lethally irradiated C57BL/6 mice were transplanted with BM with or without T cells from BALB/c mice along with luciferase-labelled C1498 mouse leukemia cells. The day of BMT was denoted as D0. Recipient mice were treated with vehicle (PBS) or rLIF (*i.p.*, 30ng/g body weight, twice a day, from D-4 to D3). **a.** Kaplan-Meier survival curve of mice. **b.** Percentage of tumor relapse in mice. **c.** Representative BLI images of mice throughout the experiment. Kaplan-Meier survival analysis was used to compare among groups. *: $p < 0.05$, ***: $p < 0.001$, n.s.: not significant.

d. Schematic illustration of the role of LIF in protecting against GVHD. The diagram was prepared by using BioRender software.

Figure 1

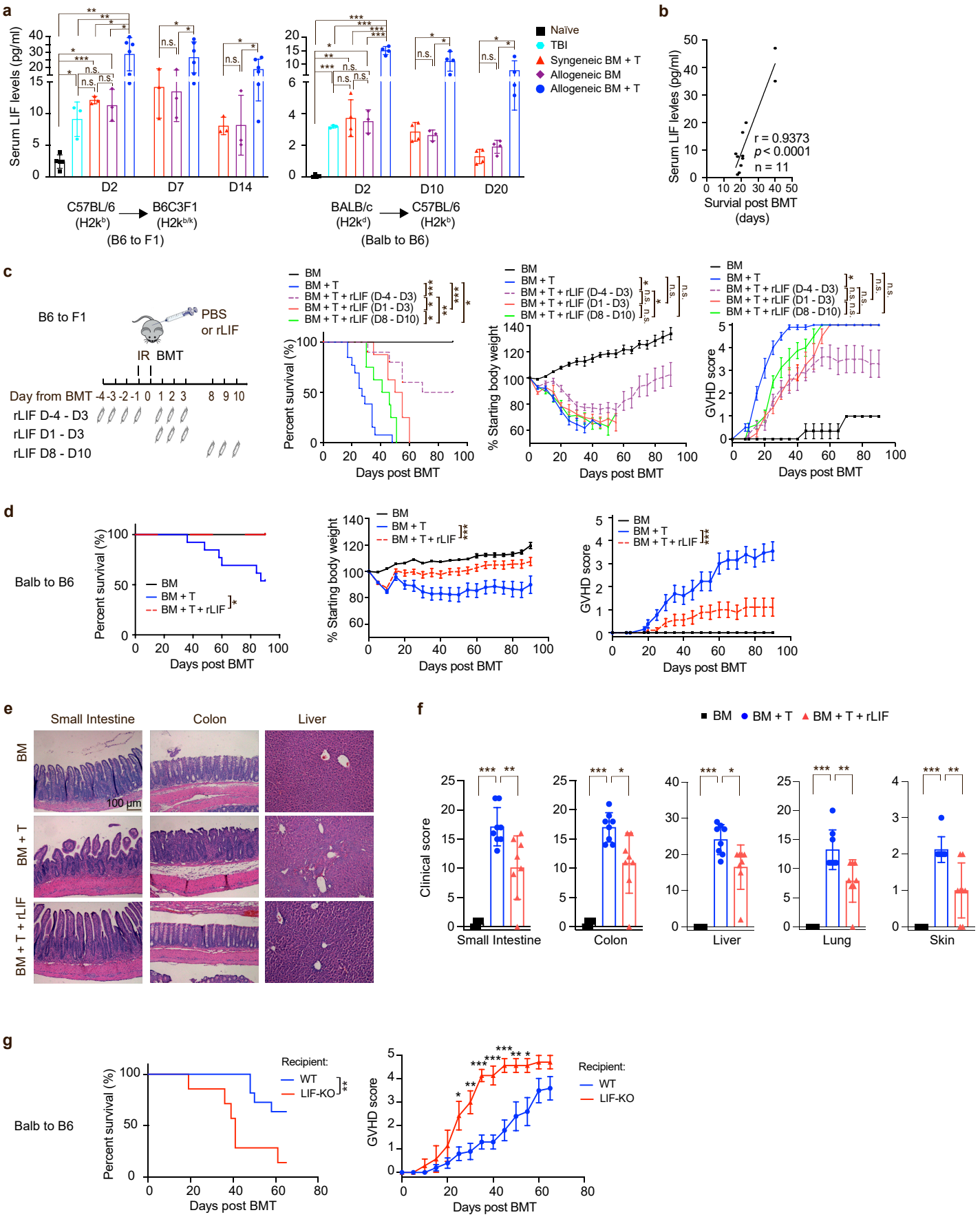
a
Serum LIF levels (pg/ml)
Naïve
TBI
Syngeneic BM + T
Allogeneic BM
Allogeneic BM + T
D2
D7
D14
C57BL/6 (H2k^b) → B6C3F1 (H2k^b/k)
(B6 to F1)
D2
D10
D20
BALB/c (H2k^d) → C57BL/6 (H2k^b)
(Balb to B6)
b
Serum LIF levles (pg/ml)
r = 0.9373
p< 0.0001
n = 11
Survial post BMT (days)
c
B6 to F1
PBS or rLIF
IR BMT
Day from BMT -4 -3 -2 -1 0 1 2 3 8 9 10
rLIF D-4 - D3
rLIF D1 - D3
rLIF D8 - D10
BM
BM + T
BM + T + rLIF (D-4 - D3)
BM + T + rLIF (D1 - D3)
BM + T + rLIF (D8 - D10)
Percent survival (%)
% Starting body weight
GVHD score
Days post BMT
d
Balb to B6
BM
BM + T
BM + T + rLIF
Percent survival (%)
% Starting body weight
GVHD score
Days post BMT
e
Small Intestine
Colon
Liver
BM
BM + T
BM + T + rLIF
100 μm
f
BM
BM + T
BM + T + rLIF
Clinical score
Small Intestine
Colon
Liver
Lung
Skin
g
Balb to B6
Recipient:
WT
LIF-KO
Percent survival (%)
GVHD score
Days post BMT

Figure 2

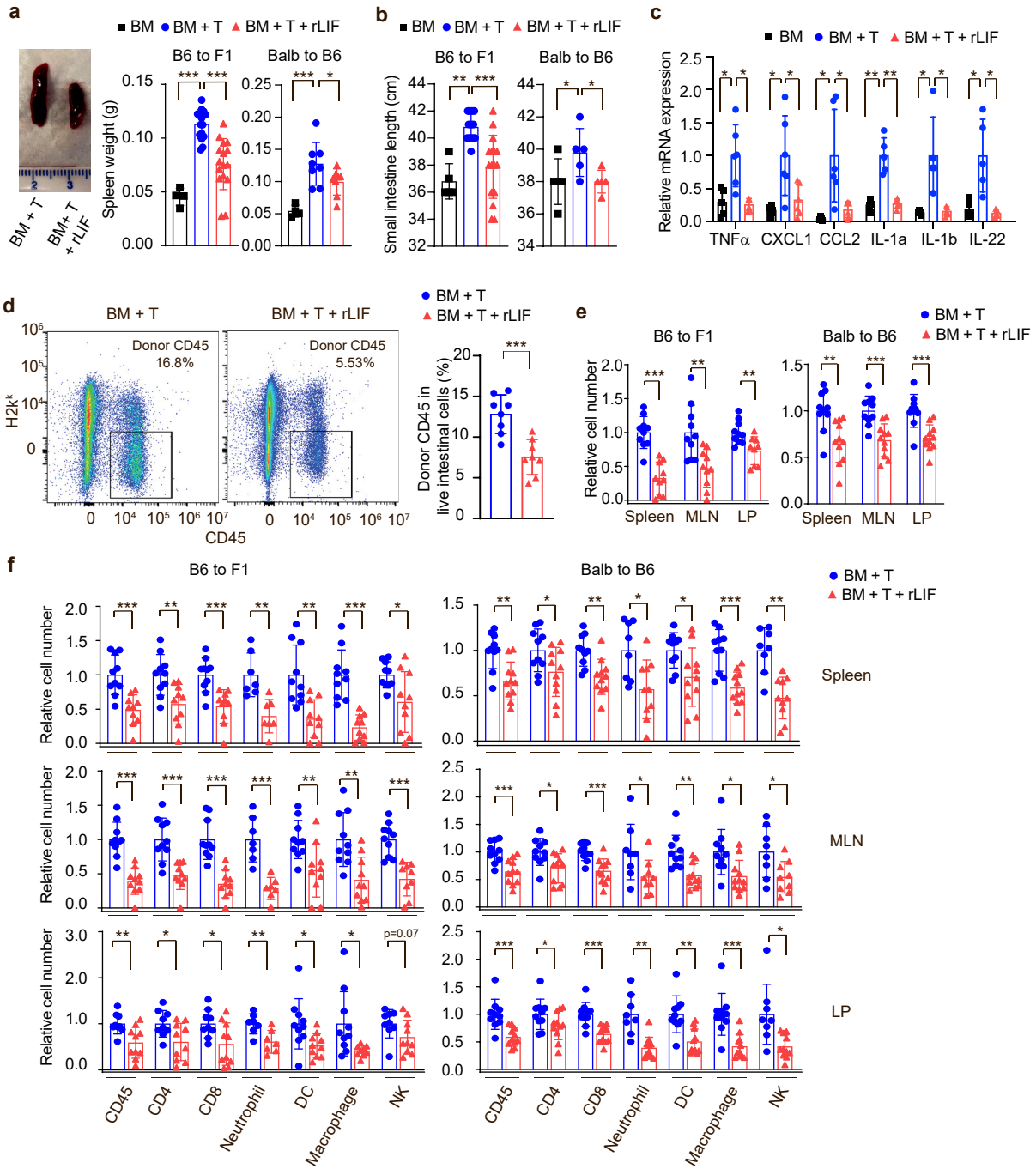
a
BM
BM + T
BM + T + rLIF
B6 to F1
Balb to B6
Spleen weight (g)
BM + T
BM+ T + rLIF
b
Small intestine length (cm)
c
Relative mRNA expression
TNFα
CXCL1
CCL2
IL-1a
IL-1b
IL-22
d
Donor CD45 16.8%
Donor CD45 5.53%
H2k^k
CD45
Donor CD45 in live intestinal cells (%)
e
Relative cell number
Spleen
MLN
LP
f
CD45
CD4
CD8
Neutrophil
DC
Macrophage
NK
p=0.07

Figure 3

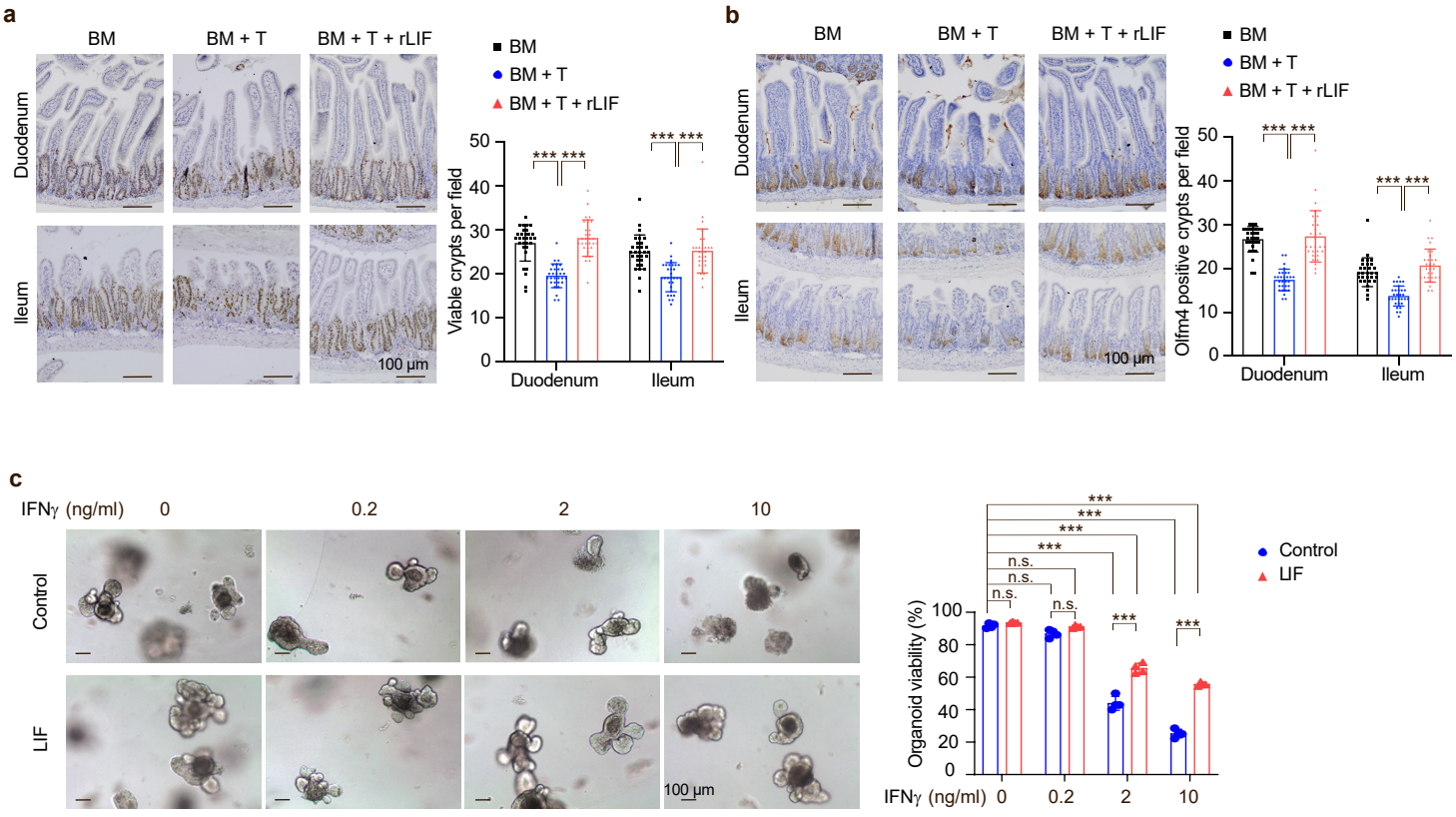
a
BM
BM + T
BM + T + rLIF
Duodenum
Ileum
100 μm
Viable crypts per field
Duodenum
Ileum
b
Olfm4 positive crypts per field
c
IFNγ (ng/ml) 0 0.2 2 10
Control
LIF
Organoid viability (%)
n.s.
Control
LIF

Figure 4

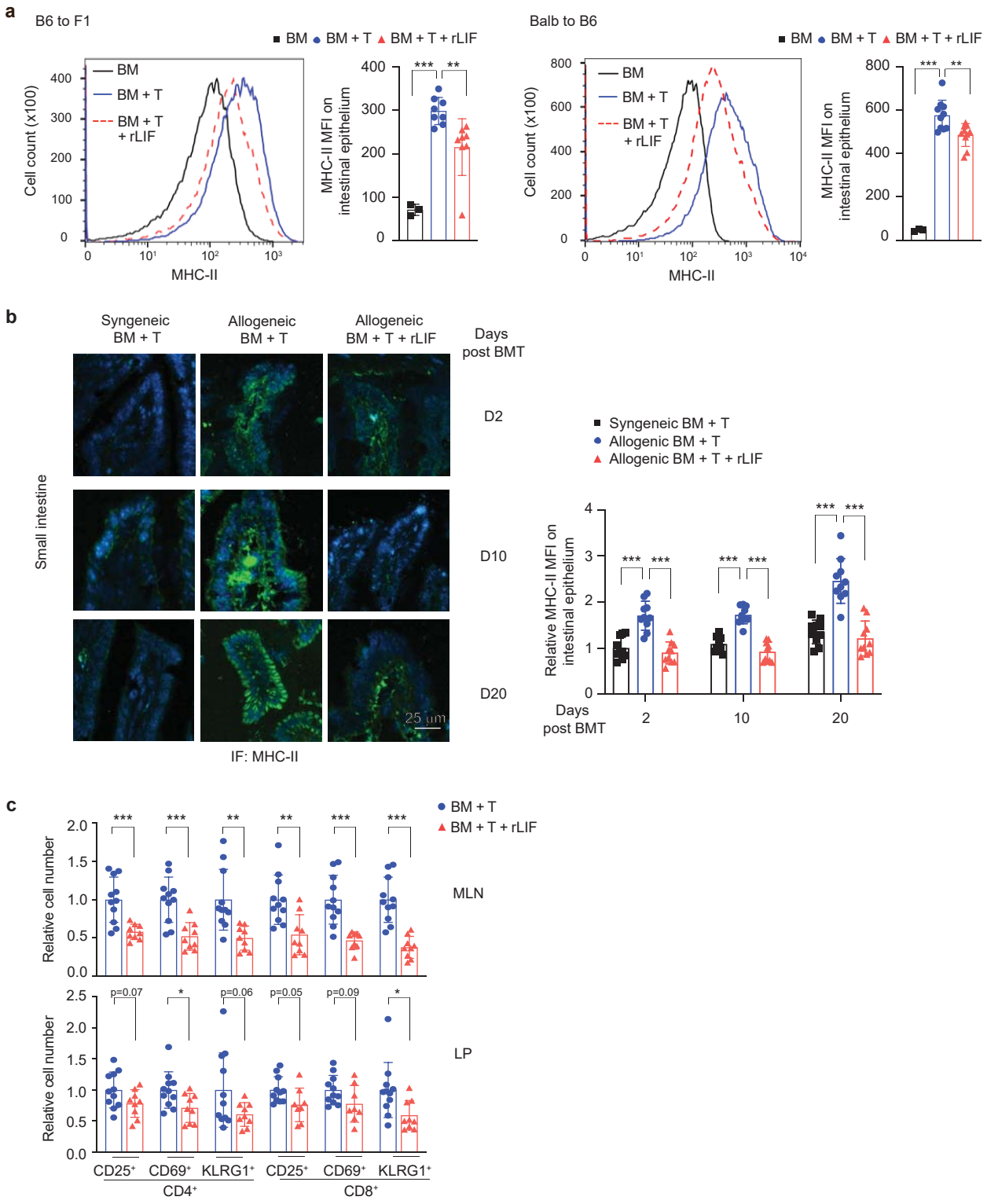
a
B6 to F1
BM
BM + T
BM + T + rLIF
Cell count (x100)
MHC-II
MHC-II MFI on intestinal epithelium
Balb to B6
b
Syngeneic BM + T
Allogeneic BM + T
Allogeneic BM + T + rLIF
Days post BMT
D2
D10
D20
Small intestine
25 µm
IF: MHC-II
Syngeneic BM + T
Allogenic BM + T
Allogenic BM + T + rLIF
Relative MHC-II MFI on intestinal epithelium
Days post BMT
c
BM + T
BM + T + rLIF
Relative cell number
MLN
LP
p=0.07
p=0.06
p=0.05
p=0.09
CD25+
CD69+
KLRG1+
CD4+
CD8+

Figure 5

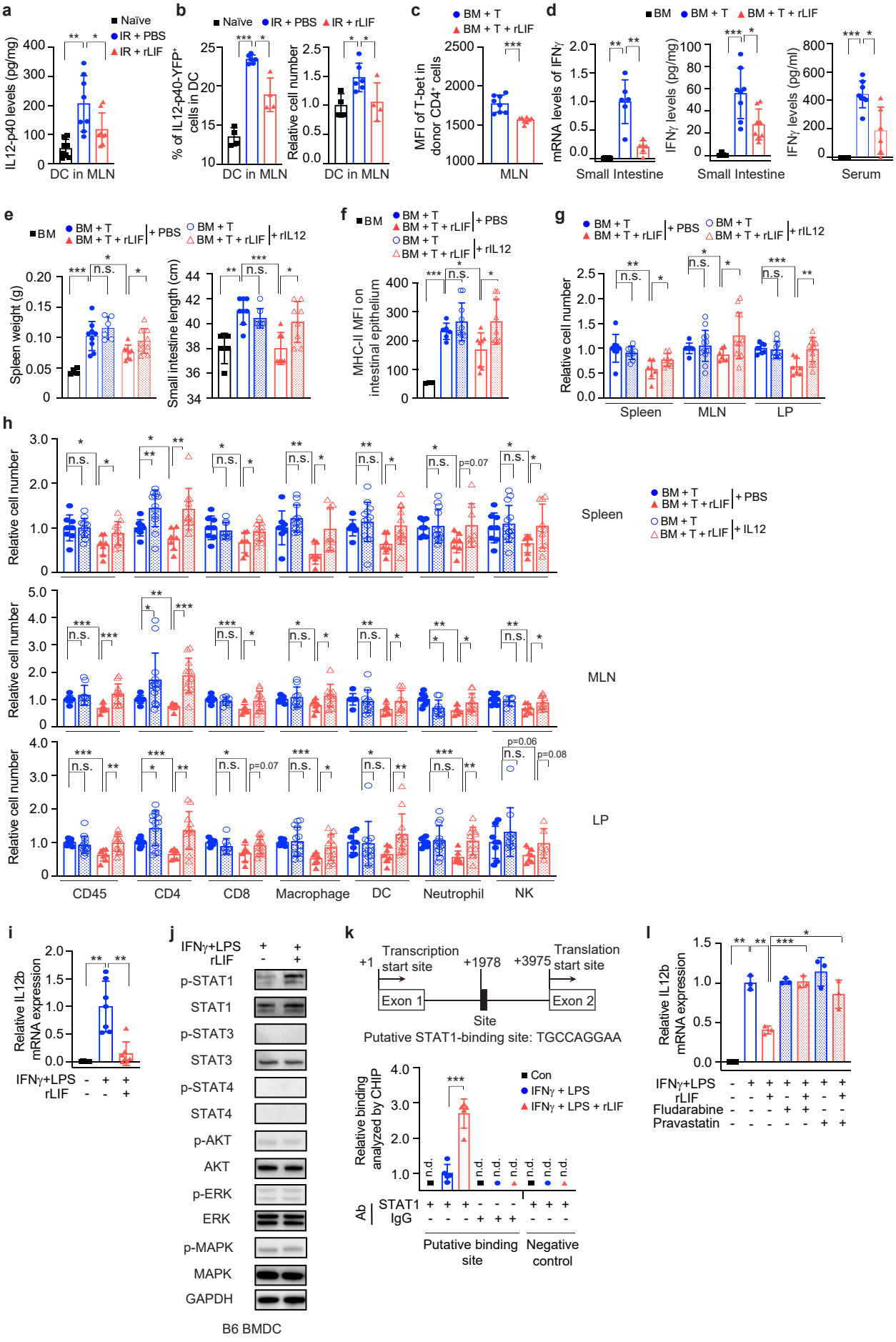
a
Naïve
IR + PBS
IR + rLIF
IL12-p40 levels (pg/mg)
DC in MLN
b
% of IL12-p40-YFP+ cells in DC
Relative cell number
c
BM + T
BM + T + rLIF
MFI of T-bet in donor CD4+ cells
MLN
d
BM
mRNA levels of IFNγ
IFNγ levels (pg/mg)
IFNγ levels (pg/ml)
Small Intestine
Serum
e
+ PBS
+ rIL12
Spleen weight (g)
Small intestine length (cm)
n.s.
f
MHC-II MFI on intestinal epithelium
g
Relative cell number
Spleen
MLN
LP
h
Relative cell number
p=0.07
p=0.06
p=0.08
CD45
CD4
CD8
Macrophage
DC
Neutrophil
NK
i
Relative IL12b mRNA expression
IFNγ+LPS
rLIF
j
IFNγ+LPS
rLIF
p-STAT1
STAT1
p-STAT3
STAT3
p-STAT4
STAT4
p-AKT
AKT
p-ERK
ERK
p-MAPK
MAPK
GAPDH
B6 BMDC
k
Transcription start site
Translation start site
+1
+1978
+3975
Exon 1
Exon 2
Site
Putative STAT1-binding site: TGCCAGGAA
Relative binding analyzed by CHIP
Con
IFNγ + LPS
IFNγ + LPS + rLIF
n.d.
Ab
STAT1
IgG
Putative binding site
Negative control
l
Relative IL12b mRNA expression
IFNγ+LPS
rLIF
Fludarabine
Pravastatin

Figure 6

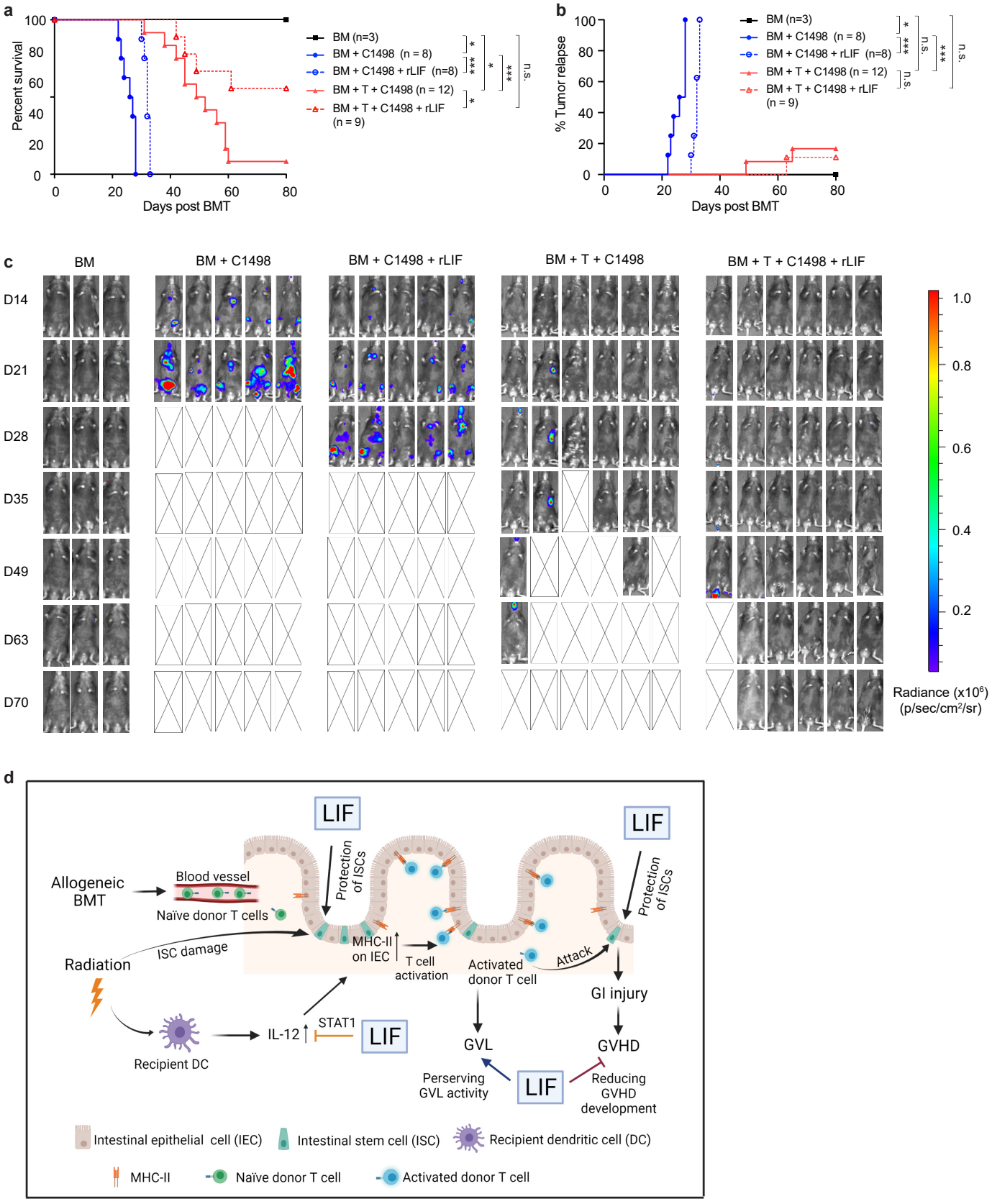
a
Percent survival
Days post BMT
BM (n=3)
BM + C1498 (n = 8)
BM + C1498 + rLIF (n=8)
BM + T + C1498 (n = 12)
BM + T + C1498 + rLIF (n = 9)
b
% Tumor relapse
Days post BMT
c
BM
BM + C1498
BM + C1498 + rLIF
BM + T + C1498
BM + T + C1498 + rLIF
D14
D21
D28
D35
D49
D63
D70
Radiance (x10⁶) (p/sec/cm²/sr)
d
LIF
Protection of ISCs
Allogeneic BMT
Blood vessel
Naïve donor T cells
Radiation
ISC damage
MHC-II on IEC
T cell activation
Activated donor T cell
Attack
GI injury
Recipient DC
IL-12
STAT1
GVL
GVHD
Perserving GVL activity
Reducing GVHD development
Intestinal epithelial cell (IEC)
Intestinal stem cell (ISC)
Recipient dendritic cell (DC)
MHC-II
Naïve donor T cell
Activated donor T cell